

Dark Energy Survey Stellar Proper Motions

Suyog Bobhate

Pennsylvania, United States

Abstract

This report aims to compile and present statistics, analytics and insights into proper motions obtained for stars from the Dark Energy Survey (DES). After looking at some initial statistics of the number of observations and velocities for each object from a sample tile, we ran matchers to match the objects to sources from the SIMBAD catalog and Gaia DR2. Spread model cuts were made to limit the data to star candidates. Thiel-Sen regression was used for outlier rejection and the final fit was calculated using Chi-squared fitting. We then applied several filters to the data to obtain a reliable set of proper motions. A queryable catalog was produced that could be used for further research. Lastly, we explore potential uses of the catalog such as the identification of dwarf galaxies and brown dwarf stars.

Keywords: DES, Proper Motion, Gaia, Milky Way, Dwarf Galaxies

1. Introduction

In this report, we aim to put together a catalog of stars from the DES Survey data with reliable proper motions. Proper motion(PM or μ) can be defined as the apparent motion of a star across the celestial sphere at right angles to the observers line of sight (The Editors of Encyclopaedia Britannica, 2013). Putting together this catalog of proper motions of stars can give us some useful insights, such as help us observe any unusual bulk motion of stars in the sky which might help in discovering dwarf galaxies and star clusters. This data can also be used to find faint stars such as white dwarfs and brown dwarfs with proper motions, which could help tell us more about stellar populations in the Milky Way. Lastly, this catalog would be open to use for other studies that might want a reliable list of stars with proper motion data obtained from the Dark Energy Survey.

2. Data

This study uses data from the Dark Energy Survey (DES), SIMBAD online database(CDS (Strasbourg), 2018) and the Gaia Data Release 2 archive. We used DES data from the DES Data Management database for images and tables of exposures. The SIMBAD database was queried by coordinates and we used lists of objects in the region to find matches. Similarly, we queried the

Gaia DR2 archive [1, 2, 3] to get a list of recorded objects in the region of interest and used these to match to objects from our DES data.

3. Preliminary analysis

We start by looking at some sample statistics from a single tile of a processed zone from the DES database. We take note of the velocities of objects against the number of times they were observed(Fig 1) and look at their distribution of velocities(Fig 2). It is also useful to consider the signal to noise ratio as shown in Fig 3. Note that velocities are noted in arcseconds per year.

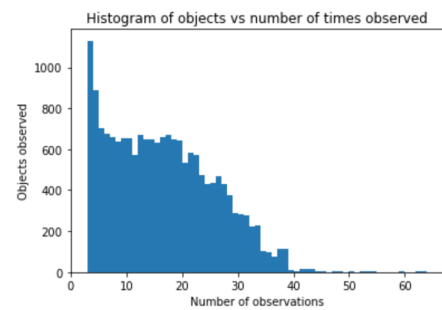


Figure 1: Histogram of velocities from tile

From Figures 1-3, we see that the results we obtain are as expected. The majority of velocities recorded

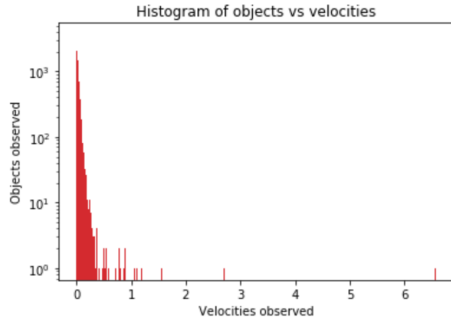


Figure 2: Logarithmic distribution of velocities

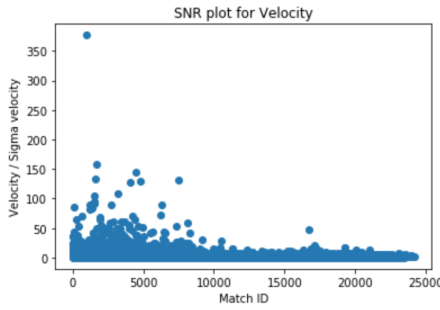


Figure 3: Signal-to-Noise ratio for velocity measurements

are relatively small with few objects having order 1 velocities. We also note from Figure 1 that most objects are observed a small number of times with the number of objects decreasing as we look for a greater number of observations.

In addition, we see that the Signal-to-Noise ratio is small for the majority of values with a fraction of objects having large SNRs.

3.1. Comparisons to SIMBAD

After studying these statistics, we matched the RA and Dec coordinates of our observed DES objects to the SIMBAD online catalog. KD-Trees were used to find the closest match with RA and Dec as the two parameters (Koegl, 2017). These matches were recorded in a table.

We found that a large number of matches were not accurate in terms of distance as there was a sizable distance between the coordinates of the DES observation and the SIMBAD coordinates. Upon inspecting some of these matches by visually comparing the positions of the DES coordinates and the matched SIMBAD object using DSS and SDSS images from the Aladin software, we found that most of the DES objects that were

observed were not present in the SIMBAD catalog and thus we were finding several false matches.

This was not unexpected as DES probes much deeper than previous surveys and a large number of the observed objects would be too faint to be previously documented. Thus we would not expect to see many of our objects in the SIMBAD compilation which uses data from previous surveys. We decided to instead run matches against the Gaia Data Release 2 objects.

3.2. Comparisons to Gaia DR2

Three tiles from 3 different zones in the DES were used to test matches against Gaia DR2 to obtain a good spread of samples and avoid any local perturbations from affecting the overall output. Similar to the SIMBAD matcher, objects were matched based on their RA and Dec coordinates using a KD-tree nearest neighbor algorithm. It was found that most Gaia objects in the region had a DES match. Figure 4 shows a plot of objects from Gaia that were matched in orange and those that were not in blue.

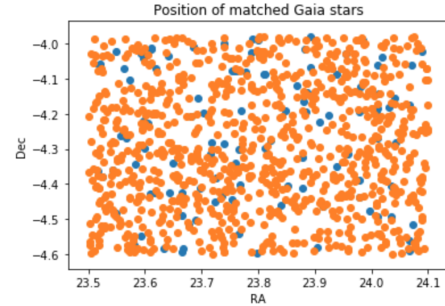


Figure 4: Positions of matched(orange) and unmatched(blue) objects for a tile

To further investigate why some objects that were clearly in the region were not matched, we decided to inspect the g-band magnitudes of these objects (Figure 5). It was reassuring to note that almost all objects with magnitudes 16-18 were matched as this is near the limit of the brightest objects DES can detect and close to the middle of Gaia's range. The objects with magnitudes brighter than 16 being unmatched is expected as these are likely too bright for DES since they oversaturate the detectors, however we expect to match all objects at magnitudes fainter than 18. From the histogram, we notice that there are around 30 objects from Gaia that are in this range but not matched to anything from the DES tile. One explanation for this could be that DES did not make enough number of reliable observations of the object for it to pass our data pruning steps. Other possible explanations include being close to a bright source

and flagged observations that are unreliable due to being on the edges of tiles (Images included in Appendix A). Figure 6 provides a plot of Gaia objects that were matched to objects in the DES data for the tile.

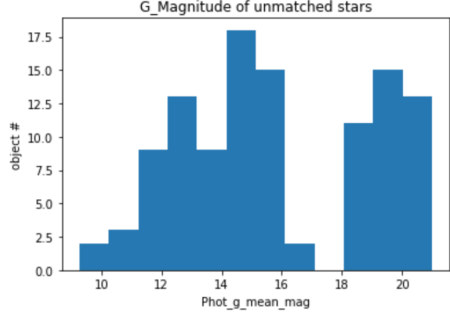


Figure 5: g band magnitudes of unmatched Gaia objects

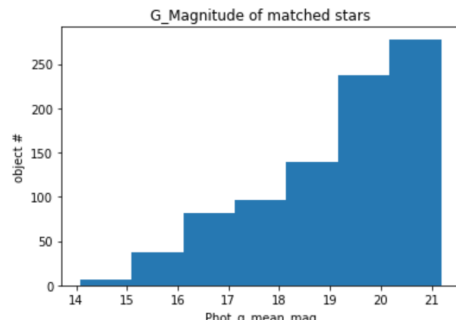


Figure 6: g band magnitudes of matched Gaia objects

We also looked at the inverse; that is the objects from the DES tile that had no matches to the Gaia data and we looked at their magnitudes. As expected, the mag-

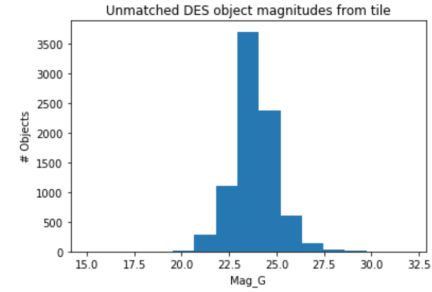


Figure 7: g band magnitudes of unmatched DES objects

nitudes of these objects are in the 20-30 range, which is much too faint for Gaia. We then proceeded to plot the Proper motions as recorded from Gaia against the

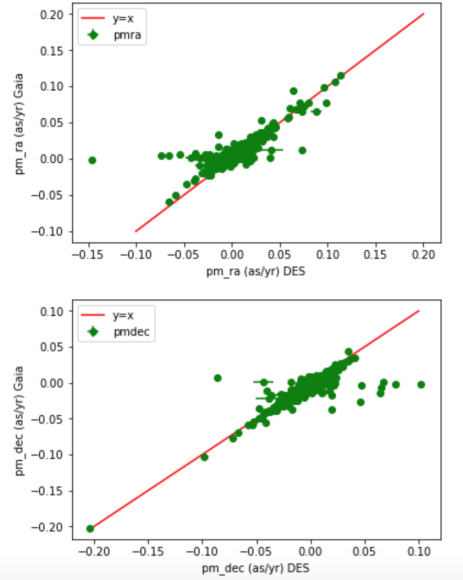


Figure 8: Proper Motions from Gaia vs DES

proper motions from DES. These plots for a single tile are shown in Figure 8.

We can see that the values largely agree and are close to the equality line, however there is some spread of values around 0 where low Gaia proper motions have high recorded proper motions from DES. A plot of the individual observations of some of these objects was made to find the cause of this deviation. Figure 9 shows one of these coordinate plots. There is a clear outlier in this plot that is causing the Proper Motion least squares fit (orange line) to be skewed. To fix this, we decided to employ a robust linear fitting model, Thiel-Sen regression, that is resistant to outliers and gives the blue line shown. Recognizing this need to include outlier rejection in our linear fitting to compute the proper motions, we decided to modify the calculation procedure. Details on this are in the next section.

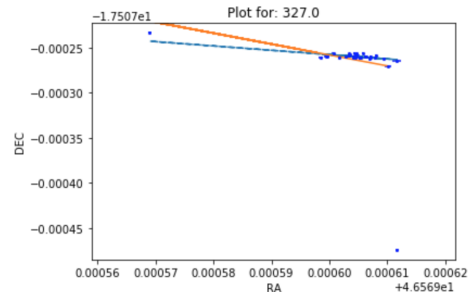


Figure 9: RA and Dec positions of object observations

3.3. Outlier Resistant Fitting

Thiel-Sen regression is a robust linear fitting method that uses the median of slopes between all pairs of points to determine the linear fit. While we did want to use this method to reject outliers, we still wanted to perform a fit with a full model of both RA and Dec proper motions using chi-square minimization. Thus the procedure was modified so that first, the median slope line was calculated using Thiel-Sen regression for RA and Dec individually. Then all points further than 3σ from the line were rejected. Then data points flagged for being near the edges of tiles and near bright stars were removed. The original chi-squared minimization fit was performed on the remaining data points. We can plot DES proper motions against Gaia proper motions again as in Fig 8 and see if the outlier rejection improved the quality of our data.

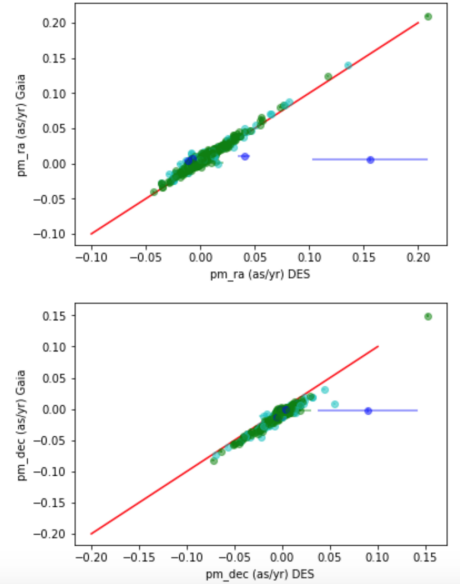


Figure 10: Gaia PMs vs DES PMs

Fig 10 shows the improved quality in our data. Blue and cyan data points in these plots resemble points that would be rejected by our reliability cuts for number of observation and goodness of fit. The green data points are the ones that will be categorized as reliable. We see that these points agree with the Gaia data barring our previously observed systematic offset.

4. Building a Proper Motion Catalog

4.1. Bulk Motion

One of the things to consider when putting together the data was to be wary of bulk motions that could skew

the values of the proper motion data. To check for effects of such bulk motions, we analyzed the proper motions obtained from Gaia of stars on different tiles. We look at statistics of these proper motions to look at effects of bulk motions. For the stars in one tile we find that the median proper motions in RA and Dec are 3.348 mas/yr and -5.615 mas/yr respectively. Comparing this to median proper motions from another tile, we see they are 4.844 mas/yr and -3.265 mas/yr. We see that there is a trend in the stellar proper motions from different parts of the sky. This is expected as we should be detecting a bulk motion of the stars in the Milky Way disk moving in the same direction. We also looked at Proper Motions of galaxies from the DES data to check for any bulk motions. Presence of these would lead us to believe that our data is offset by some amount. The median galaxy proper motions in RA and Dec are -0.005 mas/yr and 0.002 mas/yr respectively. If we compare these to the median error of the galaxy proper motions divided by the square root of n , where n is the number of objects, we find that the errors are 0.0002 mas/yr and 0.0002 mas/yr in RA and Dec respectively. These errors are not large enough to make the galaxy proper motions consistent with 0 as we would expect. This leads us to believe that there may be some offsets in the DES proper motions recorded.

A problem that arises however, is that the matched objects from the Gaia catalog for these DES galaxies only have 2-parameter Gaia solutions. Since they lack information about proper motions, we cannot compare our DES data to the Gaia data to check for offsets.

4.2. Selecting Reliable Candidates

For the final catalog, we needed to make some cuts to the data so that we would end up with a list of star candidates with reliable proper motions. The criteria are as follows:

- At least 9 observations
- Time between first and last observation of at least 100 days
- Reduced χ^2 values less than 3
- Weighted-average spread model less than 0.006
- g-band magnitude less than 24 or r-magnitude less than 23
- Signal-to-noise ratio greater than 5

The reason for including the first two cuts was that we wanted the objects in our final catalog to have sufficient number of individual observations that were taken

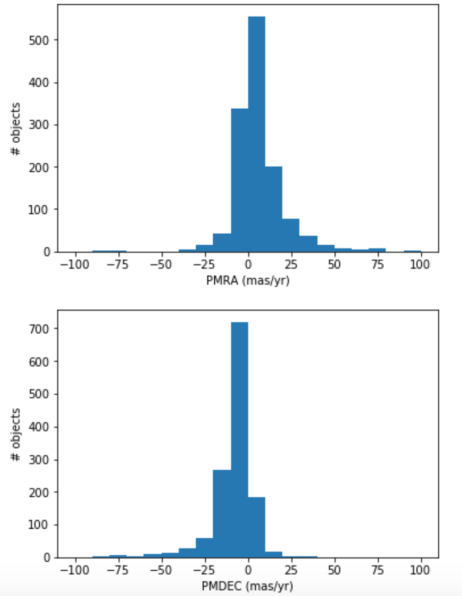


Figure 11: Proper Motions distribution for stars in a tile

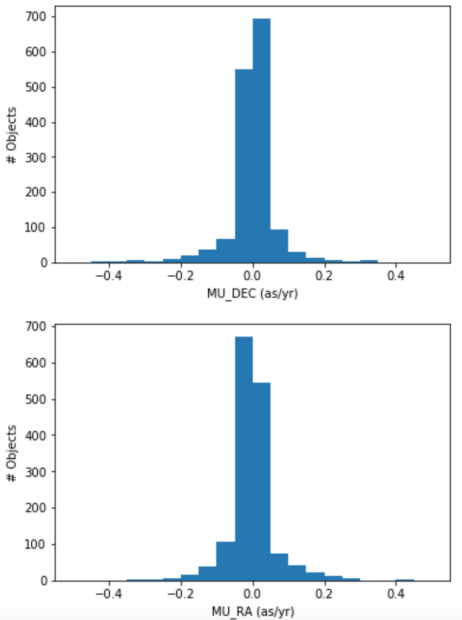


Figure 12: Proper Motions distribution for galaxies in a tile

in different observation period. This arose from an observation where we found that objects with few observations taken in a single night could have very large calculated proper motions as a result of extrapolation. The reduced χ^2 cut was included to ensure that the final objects that ended up in our catalog did not have highly non-linear motion, as we used a linear fitting model to

calculate the proper motions.

Objects with a weighted-average spread model greater than 0.006 were excluded as these would mainly be galaxies. We decided not to go with the conventional 0.003 value as some of the fainter stars could have a diffused PSF and a larger spread model.

We also decided to exclude sources with magnitudes fainter than g-band 24 as we realized that the errors on our proper motions beyond this started to spike. Figures 13 and 14 show the median errors in proper motions for Gaia and DES plotted against g-band magnitudes.

Note that the g-band in these plots refers to the 'Gaia' band used by the Gaia mission and not the SDSS g-band that DES uses. We carry out a conversion from DES g-band magnitudes to Gaia g-band magnitudes before making these plots using the color-color polynomial fittings from the Gaia Data Processing and Analysis Consortium(DPAC) (Jordi, 2018, p. 13). Thus we use a cutoff of 24th magnitude in the DES g-band as this is equivalent to approximately 22.9 magnitude in the Gaia band.

We included the r-band cut for objects that did not have observations in the g-band.

Lastly, the signal-to-noise cut was included so that we could further exclude objects with very high relative errors in their proper motions.

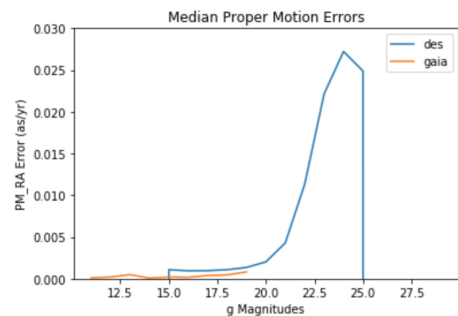


Figure 13: Median Errors in Proper Motion in Right Ascension for a tile vs g-band magnitudes

4.3. Matching Dwarf Galaxies

There were two papers by the DES Milky Way dwarf galaxies group ([4] and [5]) which were interesting to us. We wanted to see if looking at these regions would give us some bulk motion trend in the proper motions of the galaxy member stars, and if these could be used to classify them.

We selected two dwarf galaxies from the DES Y1 paper[4], namely DES J0335.65403 (Ret II) and DES J0344.34331 (Eri II) to look for in our data. Figures

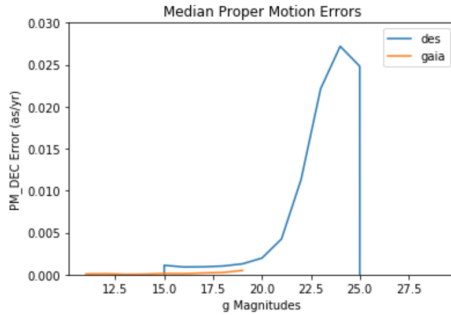


Figure 14: Median Errors in Proper Motion in Declination for a tile vs g-band magnitudes

15 and 16 show 2D density plots of the tiles containing these dwarf galaxies. As is clear from the density plots,

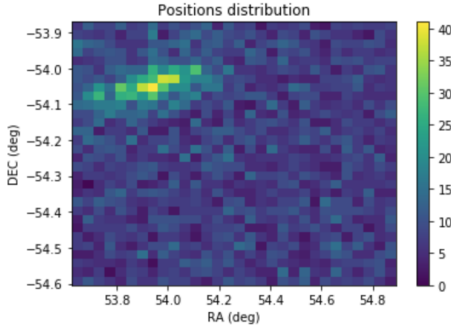


Figure 15: Position density plot of stars in tile with Ret II

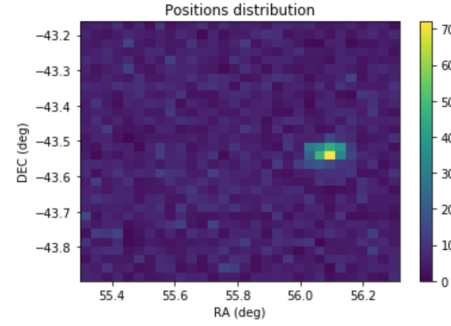


Figure 16: Position density plot of stars in tile with Eri II

there is a clear overdensity of stars in the regions where we expect to see the dwarf galaxies. This is a reaffirming confirmation of the findings in the DES Y1 paper. However, our main objective was to see if these regions had any peculiarities in the proper motions distribution that would let us identify them by looking at the proper motion data without a priori knowledge of the coordinates.

nates.

Figure 17 shows a corner plot of the distribution of proper motions in RA and Dec in the central, dense galaxy region of Eri II. The three dotted lines show quar-

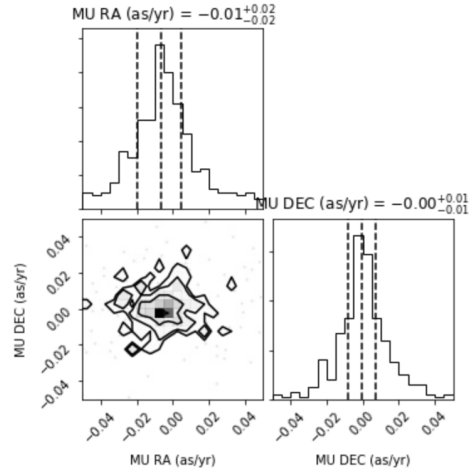


Figure 17: Corner plot of proper motion distributions in Eri II

tiles in the distribution. An important observation is the negative median of the RA proper motions, showing a skewing of the PMs in the galaxy region.

Figure 18 shows a similar plot for a larger region around the galaxy and includes a significant portion of the "background" of stars not from the overdensity. We

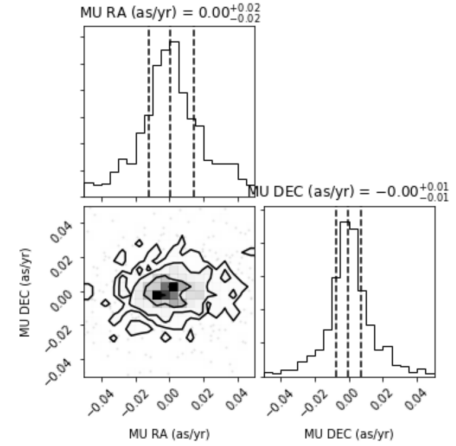


Figure 18: Corner plot of proper motion distributions around Eri II

notice that the inclusion of non-member stars shifts the median in RA PMs back to zero. We also now see two distinct dense regions in the contour plot near 0, one that is at negative μ_α and zero μ_δ and one that is near zero μ_α and μ_δ . To ensure the concentration near zero is

for the background stars, we make another contour plot of a region in the same tile but that does not include Eri II. This is shown in Fig 19.

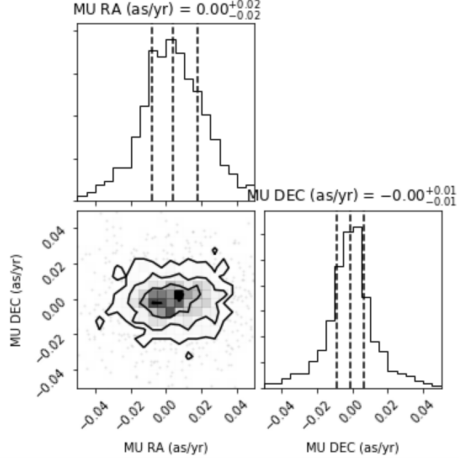


Figure 19: Corner plot of proper motion distributions of Non-member stars

4.4. Matching Brown Dwarf stars

Another topic of interest that arose was the identification of nearby brown dwarf stars with high proper motions. Our initial investigation used a list compiled by a DES collaborator (Crosell). We matched 22 dwarfs from this list with PM data from 2MASS-WISE surveys to DES data to compare PM values. The results were largely consistent within error bars within 1 to 2σ .

We noted however, that given the faintness of brown dwarfs, these sources must be fairly close for us to detect them, which would explain their high proper motions. However, this would also mean that it is very likely for them to have high parallaxes and that ignoring the effects of parallax in our proper motion fitter might be causing the disagreements in our values with those from Gaia and 2MASS-WISE.

5. Conclusions

Through this paper, we saw the methodology behind generating a reliable proper motion catalog from the DES Y4A1 data. We compared our results with existing data from previous surveys (SIMBAD) and the recent Gaia Data Release 2 data. We explored possible reasons for disagreements in these data and ways to improve our processing. Criteria for pruning of the DES data for our catalog were determined. Lastly, we explored some potential applications of our catalog.

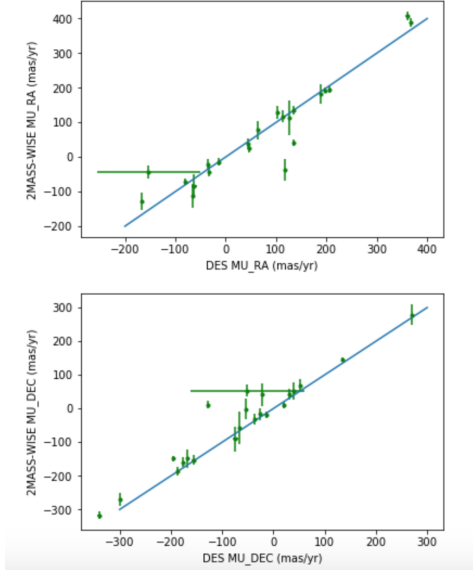


Figure 20: μ_α and μ_δ comparison between 2MASS-WISE and DES data

With the querying functions designed, once processing of all the DES Y4A1 data is complete, we should be able to query any region of the Y4A1 footprint for proper motion sources. The querying functions also include limited functionality to match to Gaia data in certain regions and to match brown dwarf candidates to our data. Nevertheless there is still room for improvement in our catalog. One improvement would be the inclusion of parallaxes in our proper motions calculation. Another improvement would be to determine if there exist any systematic errors in our data and calculate zero-point offsets and offsets with Gaia for the entire DES footprint and correct for them. Other improvements could include further refinement of our filter criteria and ways to exclude regions around extremely bright sources.

6. Acknowledgements

This work has been produced with the support of Bernstein, Eckert and Bernardinelli from the University of Pennsylvania Department of Physics and Astronomy. This work makes use of data from the Dark Energy Survey Collaboration. This work has made use of data from the European Space Agency (ESA) mission *Gaia* (<https://www.cosmos.esa.int/gaia>), processed by the *Gaia* Data Processing and Analysis Consortium (DPAC, <https://www.cosmos.esa.int/web/gaia/dpac/consortium>). Funding for the DPAC has been provided by national institu-

tions, in particular the institutions participating in the *Gaia* Multilateral Agreement.

7. References

- [6] CDS (Strasbourg). (2018). SIMBAD Astronomical Database - CDS (Strasbourg). Retrieved July 16, 2018, from <http://simbad.u-strasbg.fr/simbad/>
- [7] The Editors of Encyclopaedia Britannica. (2013, September 4). Proper motion — astronomy. Retrieved July 16, 2018, from <https://www.britannica.com/science/proper-motion>
- [8] Koegl, S. (2017, October 19). *stefankoegl/kdtree*. Retrieved June 1, 2018, from <https://github.com/stefankoegl/kdtree>
- [1] G. Collaboration, The gaia mission (2016).
- [2] L. Lindegren, J. Hernandez, A. Bombrun, S. Klioner, U. Bastian, M. Ramos-Lerate, A. de Torres, H. Steidelmuller, C. Stephenson, D. Hobbs, U. Lammers, M. Biermann, R. Geyer, T. Hilger, D. Michalik, U. Stampa, P. J. McMillan, J. Castaneda, M. Clotet, G. Comoretto, M. Davidson, C. Fabricius, G. Gracia, N. C. Hambly, A. Hutton, A. Mora, J. Portell, F. van Leeuwen, U. Abbas, A. Abreu, M. Altmann, A. Andrei, E. Anglada, L. Balaguer-Nunez, C. Barache, U. Becciani, S. Bertone, L. Bianchi, S. Bouquillon, G. Bourda, T. Brusemeister, B. Bucciarelli, D. Busonero, R. Buzzi, R. Cancelliere, T. Carlucci, P. Charlot, N. Cheek, M. Crosta, C. Crowley, J. de Bruijne, F. de Felice, R. Drimmel, P. Esquej, A. Fienga, E. Fraile, M. Gai, N. Garralda, J. J. Gonzalez-Vidal, R. Guerra, M. Hauser, W. Hofmann, B. Holl, S. Jordan, M. G. Lattanzi, H. Lenhardt, S. Liao, E. Licata, T. Lister, W. Loffler, J. Marchant, J. M. Martin-Fleitas, R. Messineo, F. Mignard, R. Morbidelli, E. Poggio, A. Riva, N. Rowell, E. Salguero, M. Sarasso, E. Sciacca, H. Siddiqui, R. L. Smart, A. Spagna, I. Steele, F. Taris, J. Torra, A. van Elteren, W. van Reeven, A. Vecchiato, Gaia data release 2: The astrometric solution, 2018.
- [3] G. Collaboration, A. G. A. Brown, A. Vallenari, T. Prusti, J. H. J. de Bruijne, C. Babusiaux, C. A. L. Bailer-Jones, Gaia data release 2. summary of the contents and survey properties, 2018.
- [4] T. D. Collaboration, K. Bechtol, A. Drlica-Wagner, E. Balbinot, A. Pieres, J. D. Simon, B. Yanny, B. Santiago, R. H. Wechsler, J. Frieman, A. R. Walker, P. Williams, E. Rozo, E. S. Rykoff, A. Queiroz, E. Luque, A. Benoit-Levy, D. Tucker, I. Sevilla, R. A. Gruendl, L. N. da Costa, A. F. Neto, M. A. G. Maia, T. Abbott, S. Allam, R. Armstrong, A. H. Bauer, G. M. Bernstein, R. A. Bernstein, E. Bertin, D. Brooks, E. Buckley-Geer, D. L. Burke, A. C. Rosell, F. J. Castander, R. Covarrubias, C. B. D'Andrea, D. L. DePoy, S. Desai, H. T. Diehl, T. F. Eifler, J. Estrada, A. E. Evrard, E. Fernandez, D. A. Finley, B. Flaugher, E. Gaztanaga, D. Gerdes, L. Girardi, M. Gladders, D. Gruen, G. Gutierrez, J. Hao, K. Honscheid, B. Jain, D. James, S. Kent, R. Kron, K. Kuehn, N. Kuropatkin, O. Lahav, T. S. Li, H. Lin, M. Makler, M. March, J. Marshall, P. Martini, K. W. Merritt, C. Miller, R. Miquel, J. Mohr, E. Neilsen, R. Nichol, B. Nord, R. Ogando, J. Peoples, D. Petracick, A. A. Plazas, A. K. Romer, A. Roodman, M. Sako, E. Sanchez, V. Scarpine, M. Schubnell, R. C. Smith, M. Soares-Santos, F. Sobreira, E. Suchyta, M. E. C. Swanson, G. Tarle, J. Thaler, D. Thomas, W. Wester, J. Zuntz, Eight new milky way companions discovered in first-year dark energy survey data (2015).
- [5] T. D. Collaboration, A. Drlica-Wagner, K. Bechtol, E. S. Rykoff, E. Luque, A. Queiroz, Y. Y. Mao, R. H. Wechsler, J. D. Simon, B. Santiago, B. Yanny, E. Balbinot, S. Dodelson, A. F. Neto, D. J. James, T. S. Li, M. A. G. Maia, J. L. Marshall, A. Pieres, K. Stringer, A. R. Walker,

The KD-Tree software library used is under Copyright (c) Stefan Kgl < *stefan@skoegl.net* > The following fair use disclaimer is included with use of the software: THE SOFTWARE IS PROVIDED "AS IS" AND THE AUTHOR DISCLAIMS ALL WARRANTIES WITH REGARD TO THIS SOFTWARE INCLUDING ALL IMPLIED WARRANTIES OF MERCHANTABILITY AND FITNESS. IN NO EVENT SHALL THE AUTHOR BE LIABLE FOR ANY SPECIAL, DIRECT, INDIRECT, OR CONSEQUENTIAL DAMAGES OR ANY DAMAGES WHATSOEVER RESULTING FROM LOSS OF USE, DATA OR PROFITS, WHETHER IN AN ACTION OF CONTRACT, NEGLIGENCE OR OTHER TORTIOUS ACTION, ARISING OUT OF OR IN CONNECTION WITH THE USE OR PERFORMANCE OF THIS SOFTWARE.

T. M. C. Abbott, F. B. Abdalla, S. Allam, A. Benoit-Levy, G. M. Bernstein, E. Bertin, D. Brooks, E. Buckley-Geer, D. L. Burke, A. C. Rosell, M. C. Kind, J. Carretero, M. Crocce, L. N. da Costa, S. Desai, H. T. Diehl, J. P. Dietrich, P. Doel, T. F. Eifler, A. E. Evrard, D. A. Finley, B. Flaugher, P. Fosalba, J. Frieman, E. Gaztanaga, D. W. Gerdes, D. Gruen, R. A. Gruendl, G. Gutierrez, K. Honscheid, K. Kuehn, N. Kuropatkin, O. Lahav, P. Martini, R. Miquel, B. Nord, R. Ogando, A. A. Plazas, K. Reil, A. Roodman, M. Sako, E. Sanchez, V. Scarpine, M. Schubnell, I. Sevilla-Noarbe, R. C. Smith, M. Soares-Santos, F. Sobreira, E. Suchyta, M. E. C. Swanson, G. Tarle, D. Tucker, V. Vikram, W. Wester, Y. Zhang, J. Zuntz, Eight ultra-faint galaxy candidates discovered in year two of the dark energy survey (2015).

Appendix A. Images of Observations

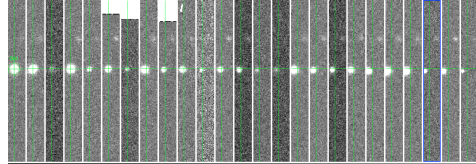


Figure A.21: All band observations of object with reliable Proper Motions

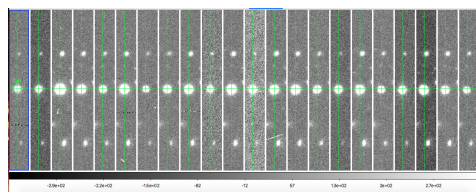


Figure A.22: All band observations of object with reliable Proper Motions

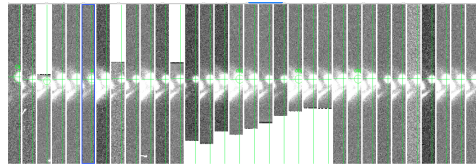


Figure A.23: All band observations of outlier

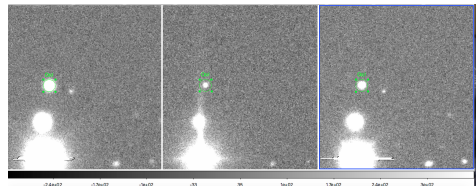


Figure A.24: All band observations of outlier

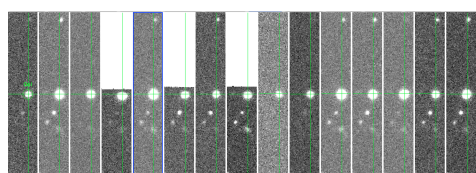


Figure A.25: All band observations of outlier